

The Optical Gravitational Lensing Experiment . Difference Image Analysis of LMC and SMC Data. The Method

K. Zebun^{1,2}, I. Soszynski^{1,2} and P.R.
Wozniak^{2,3}

¹ Warsaw University Observatory, Al. Ujazdowskie 4, 00-478 Warsaw, Poland
e-mail: (zebrun,soszynski)@astrouw.edu.pl

² Princeton University Observatory, Princeton, NJ 08544-1001, USA

³ Los Alamos National Observatory, MS-D 436, Los Alamos NM 85745, USA
e-mail: wozniak@lanl.gov

ABSTRACT

We describe the Difference Image Analysis (DIA) algorithms and software used to analyze four years (1997-2000) of OGLE-II photometric monitoring of the Magellanic Clouds, the calibration, the photometric error analysis and the search for variable stars. A preliminary analysis of photometric errors is based on the old LMC-SC2. A full catalog of more than 68 000 variable stars is presented in a separate publication.

Techniques: photometric { Methods: data analysis { Magellanic Clouds

1 Introduction

The Optical Gravitational Lensing Experiment (OGLE) (Udalski, Kubiak and Szymanski 1997) is a long term observing project which the original goal was a search for dark matter in our Galaxy using microlensing phenomena (Paczynski 1986). During more than 8 years of project duration (OGLE-I: 1992-1995, and OGLE-II: 1997-2000) a huge number of images of the densest fields like the Galactic bulge, Magellanic Clouds, Galactic disk were collected. A modified DOPHOT package (Schechter, Mateo and Saha 1993) was used to derive photometry for millions of stars. The advantages of DOPHOT are the speed and high efficiency for dense star fields, such as those observed by the OGLE project.

Most fields observed by OGLE are very crowded. In such fields very often more than one star contributes to the total light within a single observed Point Spread Function (PSF). In many cases variability refers to one of several components of the PSF, i.e., only some part of the total measured flux is due to the variable star. Therefore, the photometry of a variable star is often biased by a blending star(s).

Image subtraction can solve many of the problems described above. The method was introduced in the 90's. Two algorithms have been successfully applied: Fourier division (Tomanev and Crots 1996, Alcock et al. 1999) and a

Based on observations obtained with the 1.3-m Warsaw telescope at Las Campanas Observatory of the Carnegie Institution of Washington.

linear kernel decomposition in real space (Alard and Lupton 1998, Alard 2000). The latter algorithm was also implemented by Wozniak (2000, hereafter Paper I) in the Difference Image Analysis (DIA) package. In this paper we will use the software and nomenclature introduced in Paper I. We describe our modifications of the DIA technique, as applied to the 11 SMC and 21 LMC fields observed by OGLE-II in 1997-2000. The full catalog of variable stars in all these fields is presented in another paper (Zebur et al. 2001).

2 Observational Data

We used the data obtained during four observing seasons of the OGLE-II project: from January 1997 until May 2000. The data were collected with the 1.3-m Warsaw telescope at the Las Campanas Observatory, which is operated by the Carnegie Institution of Washington. The telescope was equipped with the "first generation" camera with a SITe 2048 × 2048 CCD detector. The pixel size was 24 μ m giving the 0.417 arcsec/pixel scale. The observations were conducted in the drift-scan "slow mode" with the gain 3.8e⁻/ADU and readout noise 5.4e⁻. Single frame's size is 2048 × 8192 pixels and corresponds to 14.2° × 57.0° in the sky. The details of the instrumentation setup can be found in Udalski, Kubiak and Szymanski (1997).

More than 60 fields were observed in the Magellanic Clouds. Each of them covered approximately 0.22 square degrees in the sky. We analyzed only frequently observed fields, 21 in the LMC and 11 in the SMC. About 400 I-band observations were collected for each of the LMC fields, and about 300 I-band observations for each of the SMC fields. For each of the LMC and SMC fields about 40 and 30 observations in the V and B-band, respectively, were also collected. The effective exposure time was 237, 173 and 125 seconds for B, V and I-band, respectively. Mean seeing of the entire data set was about 1.034.

During the DIA analysis we used all collected I-band observations, regardless of seeing. The data were standardized by the standard OGLE procedure (Udalski, Kubiak and Szymanski 1997). Uncompressed raw I-band images filled almost 400 GB of disk space.

On the reference frames (see Section 3) we detected a total of about 2×10^7 objects. The total number of photometric measurements for these objects was over 6×10^9 . The DIA analysis provided over 8×10^4 candidates for variable stars. After removing various artifacts (see Section 7) we were left with about 7×10^4 candidates. All these stars are presented in the catalog (Zebur et al. 2001).

3 Data Analysis

We used the DIA data pipeline that is based on the recently developed image subtraction algorithm described by Alard and Lupton (1998) and Alard (2000). The software package that uses this method and pipeline scheme was developed

by Wozniak (2000) and is described in Paper I.

Following Paper I, a special attention was paid to the selection of frames for preparation of the reference image. We selected frames with the best seeing, small relative shifts, low background, and free of satellite trails and other artifacts. Most cosmic rays were removed in the process of averaging of the reference image. In Section 4 we describe some modifications to that part of the original package. A weighted average of 20 best frames was adopted as the reference image. This image is used to obtain the DC signal, also known as the reference flux, for the DIA photometry. The reference frame has the same coordinate grid as the OGLE template for easy comparisons between standard OGLE and DIA databases. We also kept the original partitioning into 4 × 4 subframes, 512 × 128 pixels each.

For the actual difference photometry we adopted the script `Pipe` as presented in Paper I. A long list of input parameters required only minor adjustments between the Galactic bulge and the Magellanic Clouds data. Also the search for variables is basically the one from Paper I, except for the removal of the most obvious artifacts (see Section 7).

We found that the number of detected variables is very sensitive to one of the pipeline parameters, namely `CORR-PSF`, which sets the minimum required value for the correlation coefficient with the PSF for a candidate group of variable pixels. For details see Section 3.9 of Paper I. Lower values obviously generate more candidate variable objects. Changing `CORR-PSF` from 0.7 to 0.6 will result in about 30% longer list of objects, unfortunately with increasing proportion of artifacts. In Section 7 we briefly describe problems of selecting the optimal parameter values. All results presented in the catalog (Zebur et al. 2001) were obtained with `CORR-PSF` of 0.7, with the exception of `LMC_SC2`, where experimentally we used `CORR-PSF` = 0.6.

The tools for reliable DC photometry are still not included with any of the DIA software packages. Although we describe here the DIA results, some measurements, especially for calibration purposes, had to be made with proper photometry package like `DOPHOT`. We compare our results with OGLE data, which were also processed with the `DOPHOT` package. To avoid confusion, we list below some introduced abbreviations.

OGLE `DOPHOT` { refers to the results with the standard `DOPHOT` pipeline in OGLE, as described by Udalski, Kubiak and Szymanski (1997),
 DIA `DOPHOT` { results from reference frames created by `Make-template` script of the DIA package processed with `DOPHOT`,
 DIA photometry (DIA) { difference photometry (AC) and simple DC photometry on the reference image obtained with the DIA package.

The resulting photometric data from DIA are expressed in linear flux units. The transformation to magnitude scale is described in Section 5. The DC flux was measured on a reference image independently with DIA package and `DOPHOT` package. The details of selection of the adopted value of DC signal for the measured star are described in Section 5.

4 Changes to the DIA Package

4.1 Cosmic Ray Killer (CRK)

Magellanic Cloud images are exposed by about 30% longer than those of the Galactic bulge observations and, as a result, the number of cosmic rays on reference images is larger. The total number of cosmic ray hits accumulated on 20 frames stacked to form a reference image can pose a significant problem for photometric processing. To remove cosmic rays from reference frames we created a special procedure, attached to the program `mstack` (cf. Paper I, Section 3.6).

We take a series of resampled frames that will be coadded to generate reference frame and analyze pixels with the same $X;Y$ coordinates. We calculate the median and (standard deviation) of all ux values to be stacked. Then we check whether the value of ux in a brightest pixel that is coadded deviates from the median by more than 50%. Such a pixel is a candidate for rejection by CRK.

For these candidate pixels we examine the median of 8 neighboring pixels. If the pixel in question is at least twice as bright as the median of its neighbors, it is marked as a cosmic ray.

The pixels marked as cosmic rays are not used to calculate the average value of a pixel on a reference frame by `mstack` program.

The effect of Cosmic Ray Killer application is shown in Fig. 1. Both images show the same subframe of the LMC-SC2 field. The left image was obtained without using CRK. Cosmic rays are rather easy to spot. One of them appears as a short line. The others are considerably brighter than their vicinity. The right image has the cosmic rays removed.

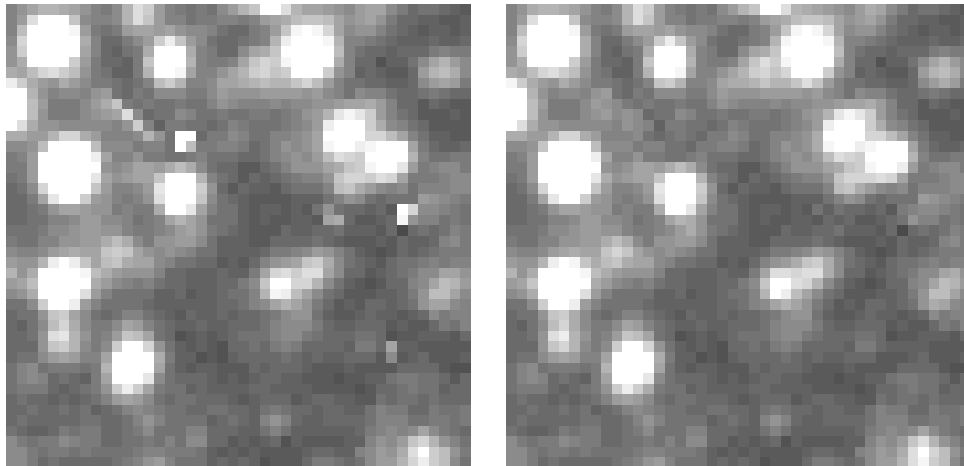


Fig. 1. Removal of cosmic rays. The same section of the reference image for LMC-SC2 field processed by standard `mstack` program (left) and our modified version (right) is shown. All clearly detectable cosmic rays are cleanly removed.

4.2 Removal of Bad Column

The CCD used by OGLE-II contained a group of bad columns. On a drift-scan they formed a line-like feature along a whole scan with a thickness of several pixels: a BAD COLUMN.

Reduction of the image includes the transformation onto a uniform coordinate grid with a bicubic spline function (cf. Paper I, Section 3.5). Near the BAD COLUMN the function strongly oscillates because it meets a group of pixels of the same large value. This results in incorrect values of flux on the transformed picture.

To remove this effect the following procedure was introduced and added to the resample program. Before applying bicubic spline interpolation we localize BAD COLUMN on the frame. Then we replace the value of the each pixel in the BAD COLUMN with an average frame background value with a random Gaussian noise superimposed. In the next step we perform a bicubic spline interpolation. Finally, we restore BAD COLUMN on a resampled frame by taking advantage of imperfect pointing and renormalizing pixel by pixel averages. Unusable values are marked as saturated and ignored later.

We also improved the quality of the results by introducing a new `sfind`, a star finding procedure. A better handling of very bright and saturated stars near the center of analyzed subframe eliminated wrong background estimates. The original version of `sfind` (Paper I, Section 3.3) calculated background value in an annulus near the center of the frame. This background was used later as a threshold for star detection. This works well when there are no very bright and saturated stars on the subframe. However bright stars are common in the Magellanic Clouds. Occasionally the original `sfind` failed because background was calculated from saturated pixels. To avoid this problem we used the median of background estimates in many locations.

5 Transformation to the Magnitude System

The Difference Image Analysis provides flux differences for variable stars. In order to convert these into more familiar magnitudes it is necessary to determine the baseline flux level (the zero point, or the DC flux), and the relation between the flux differences in DIA photometry and in DIA DOPhot photometry. As the first step to establish this relation, we determined the photometry of stars on the reference frames of all fields with DIA DOPhot. As each DIA reference image was obtained by co-adding the best 20 frames for each field, it was possible to make more accurate photometry and to reach deeper than in a single template frame used by the OGLE-II for on-line data processing: typically the number of detected stars almost doubled. The zero point for the magnitude scale on the reference image was determined by comparing stars brighter than 17.5 mag with the OGLE photometric databases (Udalski et al. 1998, 2000). The zero point was obtained separately for each of 256 segments of a reference frame.

At this point we also checked the linearity of DIA DOPhot measurements of

reference images. The differences between mean OGLE DOPHOT magnitudes of stars and DIA DOPHOT magnitudes of stars for LMC_SC2 are shown in Fig. 2 as a function of star brightness. Only the stars for which the cross-identification was better than 0.1 pixel were taken into account. It is clearly seen that co-adding twenty frames does not spoil linearity.

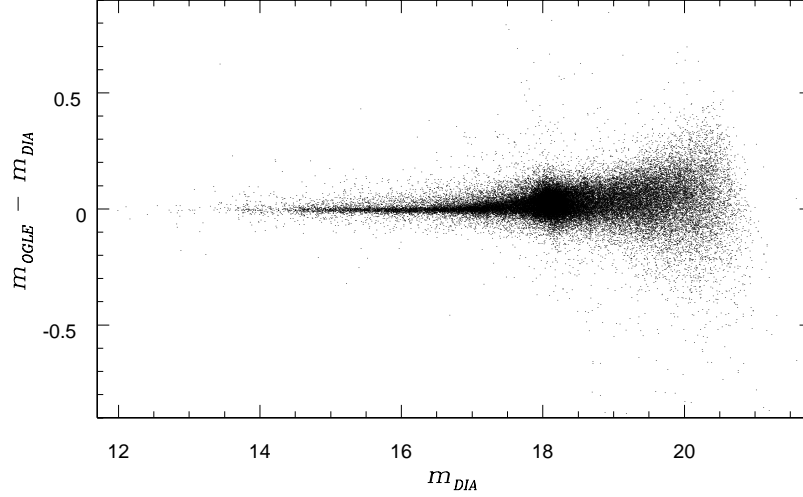


Fig. 2. Offset between the DOPHOT magnitude measured on the reference frame (m_{DIA}) and the magnitude in the OGLE database (m_{OGLE}) as a function of m_{DIA} for 50000 stars from LMC_SC2. One can see good agreement between OGLE and DIA for whole range of photometry.

The brightness, in magnitudes, of each photometric point was calculated using formula:

$$m_i = -2.5 \log(f_{DC} + a \cdot f_{ACI}) + \text{zero_point} \quad (1)$$

where: $f_{DC} = 10^{0.4(m_{DC} - m_{ref})}$ { brightness (in flux) on the reference frame, expressed in DOPHOT flux units,

f_{ACI} { difference brightness from DIA photometry,

a { coefficient scaling DIA flux to flux measured by DOPHOT,

zero_point { magnitudes zero point taken from comparison with OGLE database.

To determine the coefficient a we used two methods. The first method was described in Paper I. We used DIA photometry and DIA DOPHOT photometry obtained on a reference frame. For isolated stars the contribution of neighboring stars to the total flux is less than 1% and can be neglected.

We expressed the brightness of stars in magnitude units. The upper panel of Fig. 3 shows the relationship between I-band magnitude obtained by DIA DOPHOT and $-2.5 \log$ of DIA DC flux. The relation is obviously linear. We used the least squares method to fit a linear function. The slope is 1.004 ± 0.005 . We derived the a coefficient of Eq. (1) from the magnitude

difference (lower panel of Fig. 3) between x and y axis in the upper panel of the Fig. 3 using the relation

$$a = 10^{\text{difference}/2.5}. \quad (2)$$

The line in the lower panel of Fig. 3 is the best linear fit of the magnitude difference yielding the value of $a = 7.61 \pm 0.06$.

In the second method the coefficient a was obtained by comparing light curves of Cepheids detected in the D IA data and in the OGLE database. These stars are bright, photometry has good quality and more importantly the catalog of Cepheids has already been published by OGLE (Udalski et al. 1999a, 1999b). For each Cepheid we calculated the coefficient a by minimizing the differences between measurements for the same objects in both catalogs. In Fig. 4 we present individual estimates of the coefficient for each Cepheid. The median is $a = 7.60 \pm 0.08$, making both results consistent and in very good agreement with the value found in Paper I for the OGLE Galactic Bulge data. Field to field variations were within the 1% error given above.

As we mentioned before, f_{DC} is the DC signal flux expressed in D oPhot units. We emphasize here that the DC flux level is difficult to determine for any variable located in a crowded field, no matter which method is used for photometry. As long as there is a high probability that any given PSF is composed of a blend of several stars, with only one of them variable, there is no general way to figure out what is the DC component corresponding to the variable object. One of the few exceptions is provided by gravitational microlensing, which can be modeled as a purely geometrical effect. Another example is a light curve of a detached eclipsing binary, for which the contribution of the "third light" can be determined. But there is no general solution. The virtue of the D IA is that it presents this generic problem with full clarity, while this issue is not so obvious if a software like D oPhot is used. However, the problem is always there, hidden or not.

The DC flux measurement on a reference image from the D IA package is not very precise. This is because D IA is not modeling the star's vicinity on a reference frame and not removing nearby stars prior to calculating the flux. To minimize the problem of proper DC signal calculation we also calculated a D IA D oPhot photometry on a reference frame, which was converted to DC flux for each star detected on the reference frame using relationships derived above. At this point the best solution was to adopt D IA D oPhot flux as the correct DC signal for a variable star. However there are some caveats of this procedure. For example small differences in the DC flux, after transformation to magnitude system, result in very large differences. Fig. 5 shows two light curves of a single star from LMC_SC4 field. For these light curves we used two DC flux values that differ by 0.5 mag. It is clear that the light curves are not the same. The differences between both light curves are even as large as 6 mag.

Such wrong DC flux estimates are caused by different break up of some blends in separate runs of D oPhot and occurred in our database for about 5% of all variables. We used the following procedure to correct DC flux. After searching the D IA database for objects that could be identified on OGLE

template to better than 0.3 pixels, we compared OGLE DOPHOT and DIA photometry. When the median of differences between OGLE DOPHOT and DIA measurements was larger than 0.1 mag we adopted the more noisy but less biased DC signal from the DIA photometry.

The DIA AC signal is measured on subtracted images at the position of the variable object (see Paper I, Section 3.9). Of course the variable may be blended with a brighter star which is not resolved by DOPHOT. Therefore the variable stars are not always identified positionally with a high precision on the reference frame. We decided to set a limit of identification distance between the position of a variable star and the position of the nearest object in the DIA DOPHOT list of stars. When the distance was smaller than the limit we used the DC signal from the DIA DOPHOT photometry, otherwise we adopted as the DC signal the flux from DIA photometry on the reference image. The separation limit depended linearly on the magnitude, ranging from 4 pixels for the brightest stars to 1 pixel at the faint end. Occasionally, there was no detectable DOPHOT star on the reference frame at the location of a variable star, which usually means that the variable was above the detection threshold on some frames only, and that none of those contributed to the reference image. Some other cases were likely pseudo-variables, due to random increase of noise on some subtracted frames. In some cases we found more than one star to be closer than the adopted separation limit. In these cases we used the DC signal for the brightest of those stars.

6 Noise Properties

The DIA delivers very precise measurements of the AC signal. Therefore, light curves of variable stars are smoother than those from DOPHOT data. In this Section we assess the noise characteristics for our DIA data.

The DIA errors are affected by photon noise, but obviously they are larger. Wozniak (2000) used data for a few hundred bulge microlensing events to estimate these errors. Microlensing is very rare in the LMC and SMC, but a very similar procedure can be applied to constant stars. Wozniak (2000) fitted a point model to the microlensing event light curve and calculated standard deviation of measurements around the model in the unmodelled region, where the flux is practically constant. As most stars are constant and trivial to model, they are well suited for DIA error estimates. However this approach required slight modifications of the pipeline, by basically bypassing `getvar`, which normally only generates the list of positions for candidate variables. For noise estimates on a given frame we made the list of all detectable stars with no variables closer than 5 pixels, and supplied this directly to the `phot` procedure, which extracts the actual photometry by iterating through the PSF.

The image subtraction software is very CPU intensive, and for the first edition of the LMC and SMC variable star catalog we made only a restricted error analysis, based on one field only, LMC_SC2. In this field we detected about 6200 variable star candidates out of about 730 000 stars total (Zebur

et al. 2001). The time to perform the DIA photometry is proportional to the number of measured stars. To save the CPU time we selected eight 512×128 pixel sub-frames uniformly distributed throughout the LMC_SC2 field.

The following figures are based on the results from these subframes and include the data from about 10^5 constant star light curves. The stars were grouped into 0.5 mag bins according to the DIA DOPhot flux. In Fig. 6 we present the rms residuals around the median, normalized by photon noise (upper panel) and expressed in magnitudes σ_I (lower panel). The best fit to the data is shown as solid line and described by:

$$\frac{F}{\sigma_{ph}} = 1.1671 - (0.8 + 2.736 \times 10^{-4} F)^{1/2}; \quad (3)$$

For this fit we did not use the brightest bin where photon noise is very low and imperfections of the PSF determination dominate the residuals.

The run of σ_I is almost linear down to 18 mag. For the brightest stars ($I < 16$ mag) the errors are at the level of 0.005 mag. Then the errors grow to about 0.08 mag for stars of 19 mag and 0.3 mag for stars at $I = 20.5$ mag (OGLE photometry limit, see Fig. 2). For the transformation of the DIA fluxes (ordinate of the filled points in the upper panel) to magnitudes (ordinate of the open circles in the lower panel) we used Eq. (1).

Fig. 7 shows the distribution of residuals for selected magnitude bins. The adopted error bars were normalized using Eq. (3). The solid lines are Gaussian fits to the data. Only 1% of all measurements belong to the non-Gaussian wings, except for the very brightest stars, for which the wings are significantly larger, again, due to imperfect modeling of the PSF.

The error bars quoted in the catalog (Zebur et al. 2001) are given by the photon noise corrected with Eq. (3). The current error analysis is based on a single field, LMC_SC2, and as such should be considered preliminary.

7 The Results { Variable Objects

While selecting about 10^5 variables out of about 10^7 stars, with a typical number of about 400 photometric data points, there is no way to complete the process manually. The only option is a fully algorithmic procedure, implementing a set of filters for selecting variables and rejecting artifacts. The initial algorithm to select variables is included in program `getvar` in the DIA package (Paper I, Section 3.9). In practice there is always a trade-off between the number of admitted artifacts and missed variables. At this time we are not able to present the optimum algorithm. Most likely the optimum selection process will have to be found empirically, as it requires a very complex multiparametric optimization which takes a lot of CPU time. Nevertheless we should be getting closer to the goal through the subsequent releases of the catalog.

The present catalog basically adopts the algorithm as used in the analysis of the OGLE-II BUL_SC1 field (Paper I). The photometry for all objects from the DIA database of variable objects expressed in linear flux units as well as

in magnitudes is presented in Zebrun et al. (2001). The catalog contains many known kinds of variables, i.e., pulsators, eclipsing binaries etc, but it may still contain some artifacts.

7.1 The Artifacts

Constant stars located close to a bright star account for a significant number of artifacts. Their pseudo-variability comes from the background variations in the wings of the bright star (variable or not, because atmospheric and instrumental scattering may also induce variable wings).

To remove these artifacts we proceeded as follows. For each variable objects we calculated a cross-correlation function of light curves with every object within a 15 pixels radius. When the correlation between any two light curves was higher than a given threshold (0.7 in our case) we assumed that both stars varied in the same way. Next, we sorted the stars with similar light curves according to their brightness and identification with DIA DoPhot star on reference frame. The brightest star was marked as the true variable, and all remaining stars were treated as artifacts.

During the third observing season of OGLE-II the telescope mirror was realuminized. This had an effect on some faint stars which were close to bright stars. Some of these faint stars exhibited a sudden variability coincident in time with the aluminization. To remove these pseudo-variables from our sample we used a cross-correlation function again. First, we selected one star with such behavior in each of our fields as a template of a pseudo light curve. Next, we cross-correlated this light curve with the light curves of all stars in a given field. When any of the stars had cross correlation with our template star close to 1 or -1 we added this star to the list of suspected artifacts. Finally, we inspected by eye all these light curves and rejected many of them as artifacts.

7.2 Stars with High Proper Motion

Eyer and Wozniak (2001) recognized that pairs of variables from the catalog published by Wozniak (2000) separated by about 3 pixels were in fact single non-variable stars with a detectable proper motion. One component of a pair showed monotonic increase in brightness, while the other varied in opposite sense, with the total flux roughly constant. Hence, the two light curves had the cross correlation coefficient close to -1. We found about 1000 such pairs in the LMC and about 300 in the SMC and excluded them from the catalog of variables (Zebrun et al. 2001). Their catalog will be presented in a separate paper.

8 Summary

We described application of the DIA method to the LMC and SMC observational data. We followed very closely the procedure developed in Paper I, with minor

modifications. The catalog of variables (Zebur et al. 2001) should be considered to be the first, preliminary edition, to be gradually improved. We encourage the users to bring to our attention any problems they might encounter while using it.

OGLE-III is using a new CCD camera with 15 m pixels, corresponding to 0.25 arcsec/pixel and guided exposures. At better spatial resolution than available in OGLE-II, we are able to extract more precise signal with both Dophot and DIA photometry. The OGLE-II fields in the LMC and SMC are still observed with increased frequency. Therefore, we shall be able to obtain much better reference images in the near future and improve determinations of the DC flux. Higher quality light curves of all variables will follow.

Acknowledgements. We are indebted to Dr. B. Paczynski for many valuable discussions and support during preparation of this paper. It is a pleasure to acknowledge that this work began when two of us (KZ, IS) were visiting Department of Astrophysical Sciences at Princeton University, and one of us (PW) was a graduate student at that department. We would like to thank Dr. A. Udalski for numerous comments that substantially improved the paper. This work was partly supported by the KBN grant 5P03D 025 20 for I. Soszynski and 5P03D 027 20 for K. Zebur. Partial support was also provided by the NSF grant AST-9830314 to B. Paczynski.

REFERENCES

- Aldard, C. 2000, *Astron. Astrophys.*, 144, 363.
 Aldard, C., and Lupton, R.H. 1998, *Astrophys. J.*, 503, 325.
 Allcock, C., et al. 1999, *Astrophys. J.*, 521, 602.
 Schechter, P.L., Mateo, M., and Saha, A. 1993, *P.A.S.P.*, 105, 1342.
 Tomney, A.B., and Crots, A.P. 1996, *Astron. J.*, 112, 2872.
 Paczynski, B. 1986, *Astrophys. J.*, 304, 1.
 Udalski, A., Kubiak, M., and Szymanski, M. 1997, *Acta Astron.*, 47, 319.
 Udalski, A., Szymanski, M., Kubiak, M., Pietrzynski, G., Wozniak, P., and Zebur, K. 1998, *Acta Astron.*, 48, 147.
 Udalski, A., Soszynski, I., Szymanski, M., Kubiak, M., Pietrzynski, G., Wozniak, P., and Zebur, K. 1999a, *Acta Astron.*, 49, 223.
 Udalski, A., Soszynski, I., Szymanski, M., Kubiak, M., Pietrzynski, G., Wozniak, P., and Zebur, K. 1999b, *Acta Astron.*, 49, 437.
 Udalski, A., Szymanski, M., Kubiak, M., Pietrzynski, G., Soszynski, I., Wozniak, P., and Zebur, K. 2000, *Acta Astron.*, 50, 307.
 Wozniak, P. 2000, *Acta Astron.*, 50, 451, Paper I.
 Eyer, L., and Wozniak, P.R. 2001, *MNRAS*, 327, 601.
 Zebur, K., Soszynski, I., Wozniak, P.R., Udalski, A., Kubiak, M., Szymanski, M., Pietrzynski, G., Szewczyk, O., and Wyrzykowski, L. 2001, *Acta Astron.*, 51, 317.

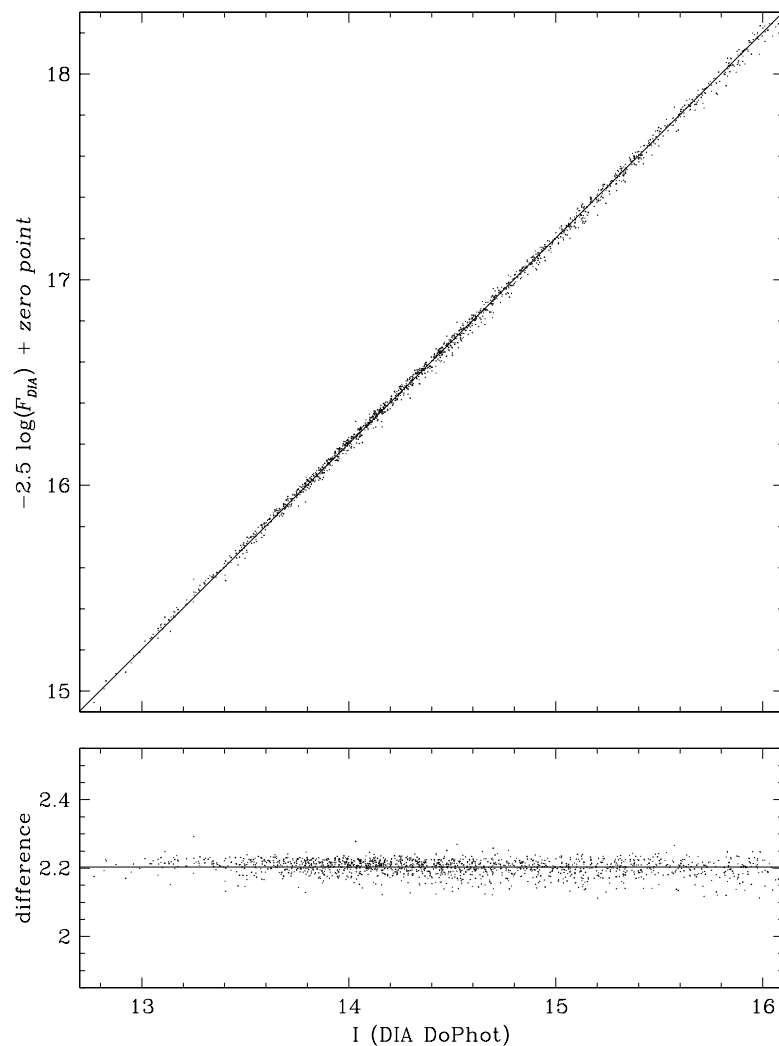


Fig. 3. First method of finding the transformation coefficient between DIA fluxes and magnitudes. I-band magnitudes measured by DIA DoPhot are plotted against the $-2.5 \log$ of the DIA DC flux (upper panel). The difference between these two magnitudes (lower panel) defines the transformation factor. The best fit gives the transformation factor of 7.61 ± 0.06 .

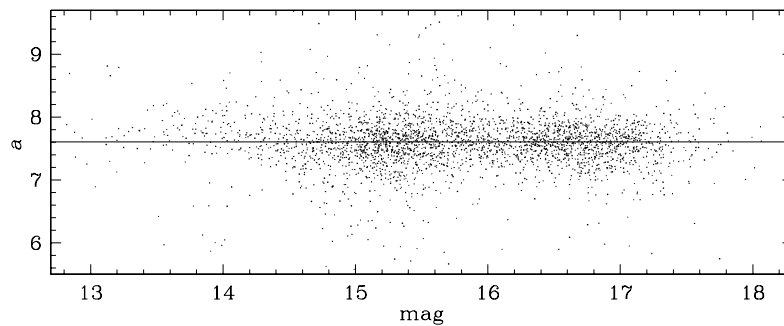


Fig. 4. Transformation coefficient from DIA flux to magnitude units calculated with Cepheid variable stars. The line corresponds to our adopted value, 7.60 ± 0.08 .

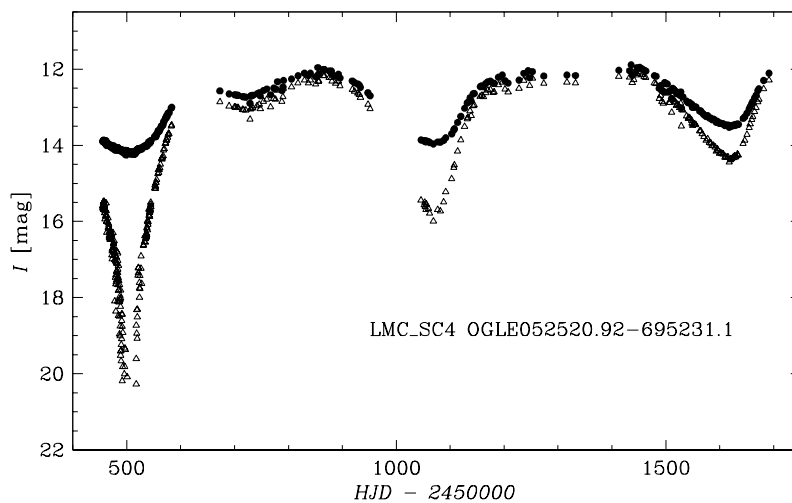


Fig. 5. Light curve of a variable star OGLE052520.92-695231.1. The difference of about 0.5 mag in DC magnitude radically changed the shape of the light curve. Full circles indicate magnitudes computed with $m_{DC} = 13.2$, and empty triangles indicate magnitudes obtained using $m_{DC} = 13.7$. The problem of wrong DC measurements applies to about 5% of all variable objects.

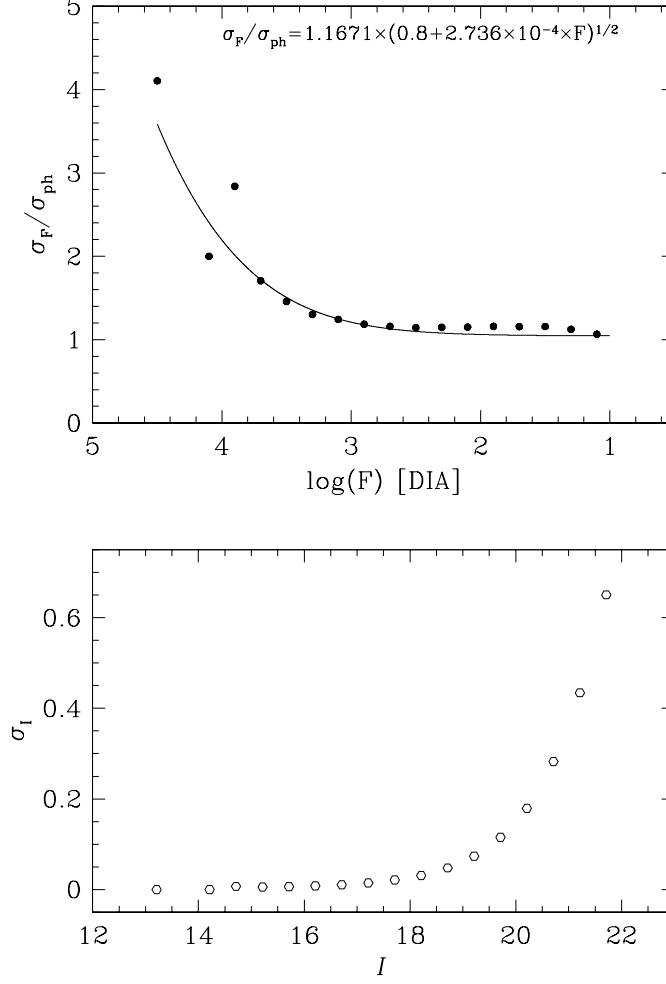


Fig. 6. In the upper panel we plot the rms scatter around the median divided by the photon noise estimate as a function of flux logarithm for a set of 32 000 constant stars from LM C_SC2 field. The flux bins correspond to 0.5 mag. The solid line is the best fit to the data points (Eq. 3). I-band magnitude error for a range of magnitudes is given in the lower panel. The open circles correspond to the points in the upper panel. The errors for the brightest stars are at the level of 0.005 mag.

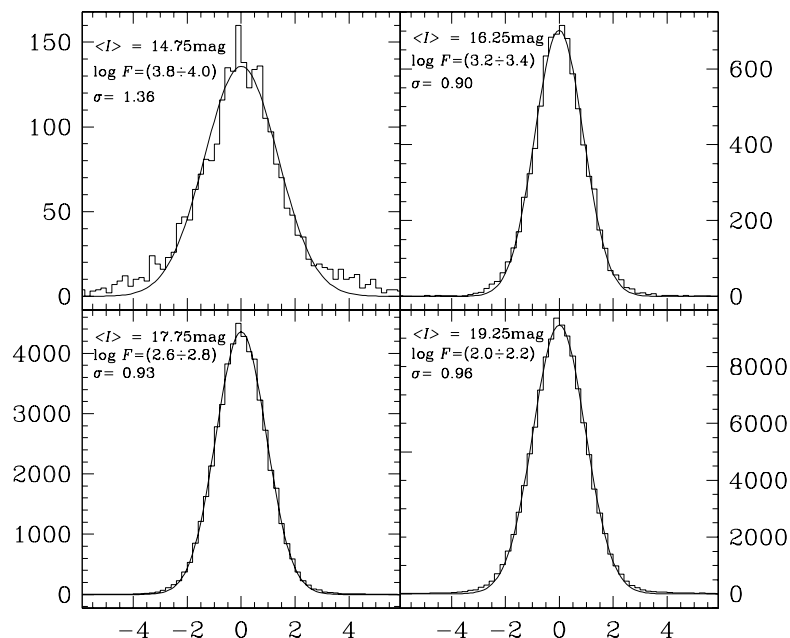


Fig. 7. Histograms of normalized residuals around median flux in four selected magnitude bins. As the normalization factor we used the photon noise corrected by the t from Eq. (3). The error distribution is well approximated by a Gaussian fit (the solid lines), with the exception of the very brightest stars, for which systematics of the PSF model are noticeable.